This is the accepted manuscript made available via CHORUS. The article has been published as:

Transverse instability and universal decay of spin spiral order in the Heisenberg model

Joaquin F. Rodriguez-Nieva, Alexander Schuckert, Dries Sels, Michael Knap, and Eugene Demler

Phys. Rev. B **105**, L060302 — Published 22 February 2022

DOI: 10.1103/PhysRevB.105.L060302

Transverse instability and universal decay of spin spiral order in the Heisenberg model

Joaquin F. Rodriguez-Nieva[1], Alexander Schuckert[2,3], Dries Sels[4,5,6], Michael Knap[2,3], Eugene Demler[6]
[1]*Department of Physics, Stanford University, Stanford, CA 94305, USA*
[2]*Department of Physics and Institute for Advanced Study, Technical University of Munich, 85748 Garching, Germany*
[3]*Munich Center for Quantum Science and Technology (MCQST), Schellingstr. 4, D-80799 München*
[4]*Department of Physics, New York University, New York, NY, USA*
[5]*Center for Computational Quantum Physics, Flatiron Institute, New York, NY, USA and*
[6]*Department of Physics, Harvard University, Cambridge, MA 02138, USA*
(Dated: November 10, 2021)

We analyze the intrinsic stability of spin spiral states in the two-dimensional Heisenberg model isolated from its environment. Our analysis reveals that the SU(2) symmetric point hosts a dynamic instability that is enabled by the existence of energetically favorable transverse deformations—both in real and spin space—of the spiral order. The instability is universal in the sense that it applies to systems with any spin number, spiral wavevector, and spiral amplitude. Unlike the Landau or modulational instabilities which require impurities or periodic potential modulation of an optical lattice, quantum fluctuations alone are sufficient to trigger the transverse instability. We analytically find the most unstable mode and its growth rate, and compare our analysis with phase space methods. By adding an easy plane exchange coupling that reduces the Hamiltonian symmetry from SU(2) to U(1), the stability boundary is shown to continuously interpolate between the modulational instability and the transverse instability. This suggests that the transverse instability is an intrinsic mechanism that hinders long-range phase coherence even in the presence of exchange anisotropy.

Characterizing the mechanisms responsible for the breakdown of phase coherence in quantum systems is a fundamental problem with broad implications in quantum science and technology. The interplay between kinetic effects, interactions, and disorder gives rise to a wide range of phase relaxation mechanisms. In the simplest scenario, the phase coherence in a superfluid is subject to the Landau criterion[1] which defines an upper limit for the superfluid velocity: when the superfluid moves faster than the sound velocity, a spatially localized defect can trigger a superfluid instability that globally destroys phase coherence[2]. In the case of a Bose-Einstein condensate (BEC) in an optical lattice with spacing a, the characteristic lattice modulation $q_{\rm l} = \pi/2a$ sets another limit for the superfluid wavevector above which a modulational instability occurs[3, 4]. Such instability can be enhanced in the presence of strong interactions[5, 6]. Rich physics and diverse mechanisms that destroy—and sometimes stabilize—the phase coherence have been discussed in the context of counterflowing superfluids[7], multicomponent[8] and spinor BECs[9–11], superconductors[12–15], in the presence of extended disorder[16–19], dipolar interactions[20–22], and driving[23–27].

Here we inquire about the fate of spin spiral states, see Fig. 1(a), in the isolated two-dimensional Heisenberg model. Such states can be created, for example, by globally rotating the spins around the x axis by an angle θ and then using a magnetic field gradient with wavevector $\boldsymbol{q}$ to rotate the spins around the z axis. Understanding the stability of spin spirals and the dynamics decay under their own internal degrees of freedom is of relevance in many important scenarios. The non-equilibrium dynamics of spin spirals has recently been in the spotlight of several cold atom experiments[28–30]. By tuning $\boldsymbol{q}$ and θ, we can tune the energy and magnetization of the system and trigger interesting far-from-equilibrium phenomena, such as quantum turbulence [31, 32], prethermalization[33], universal self-similar relaxation[34, 35], and anomalous transport[36]. In addition, the stability of spin superfluids in ferromagnetic materials, promising for dissipationless spintronic applications[37–42], hinges on the stability of long-range coherence of a spin spiral. As such, our results are useful to understand the relevant modes

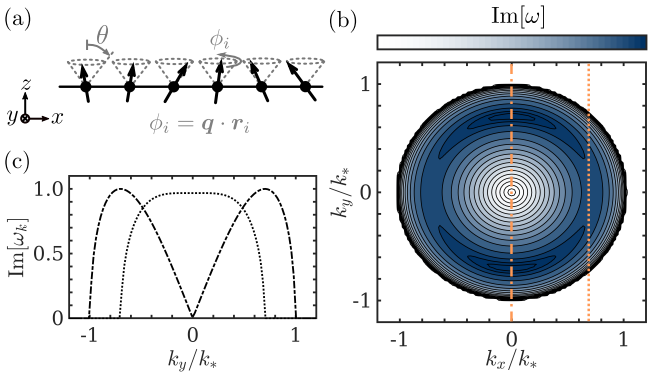


FIG. 1. (a) Schematics of a spin spiral parametrized by a wavevector $\boldsymbol{q}$ and angular amplitude θ. (b) Imaginary part of the frequency of Bogoliubov modes. The wavevectors $k_{x,y}$ are relative to $\boldsymbol{q}$, which is assumed to be pointing in the x-direction ($k_* = q\sin\theta$). The fastest growing modes are transverse to $\boldsymbol{q}$, with $k_y \approx k_*/\sqrt{2}$. (c) Slice of panel (b) plotted at the linecuts $k_x/k_* = 0$ (dotted-dashed line) and $k_x/k_* = 0.75$ (dotted line) and normalized with $1/\tau_*$ in Eq.(1). Parameters used: $\theta = \pi/4$, $q_x a = 0.5$, $q_y = 0$.

that lead to spin superfluid decay when the coupling to a thermal bath is not important.

Our analysis reveals that the SU(2) symmetry of the Hamiltonian gives rise to a dynamic instability with different characteristics from previously-studied instabilities. In particular, the instability (i) is enabled by gapless symmetry-allowed deformations of the order parameter rather than kinematic effects, (ii) is triggered by quantum fluctuations without the need for defects, disorder or a lattice, and (iii) is universal in the sense that it affects systems with arbitrary spin number S, spiral wavevector, and spiral amplitude. The main physics can be understood by noticing that the SU(2) symmetry relaxes the topological constraint that protects the U(1) phase in superfluids[37]: while in usual superfluids the thermally-activated creation of vortex-antivortex pairs or large kinematic fluctuations destroy coherence, the SU(2) symmetry alone furnishes additional 'directions' (or rotation generators) in which the phase coherence can be destroyed for arbitrary values of q (*i.e.*, the critical wavevector is zero). As indicated in Fig. 1(b), the instability evolves by unwinding the spiral via growth of modes in a ring around the wavevector $\boldsymbol{q}$. Assuming $\boldsymbol{q} = (q_x, 0)$, the fastest growing mode has transverse wavevector $k_\perp \approx k_*/\sqrt{2}$ and grows with a rate $1/\tau_*$, with

$$k_* = |\boldsymbol{q}| \sin\theta, \quad \frac{1}{\tau_*} = JS \sin^2\theta [1 - \cos(q_x a)], \tag{1}$$

until it becomes macroscopically occupied (J is the exchange coupling). In addition, numerical simulations show that the constraint $\hat{S}_j^2 = S(S+1)$ of each spin regulates the instability growth, which peaks in a time $t \approx 4\tau_*$ (largely independent of $\boldsymbol{q}$, θ, and S).

We analytically discuss dynamics in the SU(2) symmetric Heisenberg model for large S, but our conclusion are far more general. In particular, below we numerically show that the imprint of the ring of unstable modes survives even in the $S = 1/2$ limit for sufficiently small wavevectors. In addition, we show that the effect of the instability pervades away from the SU(2) symmetric point. Indeed, although it is known that the easy-plane XXZ model can host a stable superfluid state[39], we still observe a strong reduction of the critical wavevector for modulation instabilities (*i.e.*, $|\boldsymbol{q}_c| = \pi/2a$) for a wide range of values of the exchange anisotropy. As such, manifestations of the transverse instability still exist in the presence of exchange anisotropy.

Microscopic model—We consider the two-dimensional Heisenberg model on a square lattice with exchange anisotropy:

$$\hat{H} = -\sum_{\langle j,j'\rangle} J\left(\hat{S}_j^x \hat{S}_{j'}^x + \hat{S}_j^y \hat{S}_{j'}^y\right) + J_z \hat{S}_j^z \hat{S}_{j'}^z, \tag{2}$$

where $\langle j, j'\rangle$ denotes summation over nearest neighbours. Each site contains a spin S degree of freedom and periodic boundary conditions are assumed in each spatial direction. Our analysis is not affected by a Zeeman field, which is present in many relevant experiments: although a Zeeman field breaks the SU(2) symmetry of the Hamiltonian, its effect on dynamics can be removed by using a rotating frame. The initial condition is a spin spiral

$$\langle \hat{S}_j^\pm \rangle = S \sin\theta e^{\pm i \boldsymbol{q}\cdot\boldsymbol{r}_j}, \quad \langle \hat{S}_j^z \rangle = S\cos\theta, \tag{3}$$

with $\hat{S}_j^\pm = \hat{S}_j^x \pm i\hat{S}_j^y$.

Bogoliubov analysis—The equations of motion of the spin operators are given by $\partial_t \hat{\boldsymbol{S}}_j = J\sum_{j'\in\mathcal{N}_j} \hat{\boldsymbol{S}}_j \times (\hat{\boldsymbol{S}}_{j'} + \epsilon \hat{S}_{j'}^z \boldsymbol{z})$, with $\epsilon = (J_z - J)/J$, $\mathcal{N}_j$ the nearest neighbors of site j, and $\boldsymbol{z}$ a unit vector. We first analyze the linearized dynamics at short times using the approximation $\langle \hat{S}_j^\alpha \hat{S}_{j'}^\beta \rangle \approx \langle \hat{S}_j^\alpha \rangle \langle \hat{S}_{j'}^\beta \rangle$, which gives rise to the equations of motion

$$\begin{aligned} \dot{S}_j^\pm &= \mp iJ \sum_{j'\in\mathcal{N}_j} \left[(1+\epsilon) S_j^\pm S_{j'}^z - S_{j'}^\pm S_j^z\right], \\ \dot{S}_j^z &= \frac{iJ}{2} \sum_{j'\in\mathcal{N}_j} \left[S_j^+ S_{j'}^- - S_j^- S_{j'}^+\right], \end{aligned} \tag{4}$$

with $\langle \hat{S}_j^\alpha \rangle = S_j^\alpha$. Hereafter, energy and inverse time are expressed in units of JS and wavevectors in units of $1/a$. Using the initial conditions in Eq. (3), it can be shown that the solution $\bar{S}_j^\pm(t) = S\sin\theta e^{\pm i(\boldsymbol{q}\cdot\boldsymbol{r}_j + \mu t)}$, $\bar{S}_j^z = S\cos\theta$, is a steady-state solution of Eq.(4) with oscillation frequency $\mu = 2\cos\theta[(1+\epsilon)2 - \cos q_x - \cos q_y]$. Therefore, one can systematically incorporate the effects of quantum fluctuations on top of this classical stationary solution through a Bogoliubov analysis, as we discuss next.

We proceed to analyze the stability of the spiral in the isotropic exchange case, $\epsilon = 0$. We parametrize fluctuations on top of the steady-state solution using the xy components of magnetization, $S_j^\pm = \bar{S}_j^\pm + \delta S_j^\pm$; this implies that our parametrization is singular at $\theta = \pi/2$, but taking the limit $\theta \to \pi/2$ at the end still yields the correct result (a parametrization in polar coordinates that is non-singular at $\theta = \pi/2$, but more cumbersome, is discussed in the Supplement). Going into momentum space and expressing modes relative to the wavevector and frequency of the spiral, $\delta S_j^\pm = e^{\pm i(\boldsymbol{q}\cdot\boldsymbol{r}_j + \mu t)} \sum_{\boldsymbol{k}} e^{i(\boldsymbol{k}\cdot\boldsymbol{r}_j + \omega_{\boldsymbol{k}} t)} \delta S_{\boldsymbol{k}\pm\boldsymbol{q}}^\pm$, the linearized equations of motion are (see Supplement)

$$\begin{pmatrix} \omega_{\boldsymbol{k}} + \varepsilon_{\boldsymbol{q}+\boldsymbol{k}} + \frac{\Delta_{\boldsymbol{k}}}{2} - \mu & \frac{\Delta_{\boldsymbol{k}}}{2} \\ -\frac{\Delta_{\boldsymbol{k}}}{2} & \omega_{\boldsymbol{k}} - \varepsilon_{\boldsymbol{q}-\boldsymbol{k}} - \frac{\Delta_{\boldsymbol{k}}}{2} + \mu \end{pmatrix} \delta\boldsymbol{S} = 0. \tag{5}$$

Here $\delta\boldsymbol{S} = (\delta S_{\boldsymbol{q}+\boldsymbol{k}}^+, \delta S_{\boldsymbol{k}-\boldsymbol{q}}^-)^{\mathrm{t}}$, and $\varepsilon_{\boldsymbol{p}}$, $\Delta_{\boldsymbol{k}}$ are

$$\varepsilon_{\boldsymbol{q}\pm\boldsymbol{k}} = \cos\theta\,(\gamma_0 - \gamma_{\boldsymbol{q}\pm\boldsymbol{k}}), \quad \Delta_{\boldsymbol{k}} = \sin\theta\tan\theta(\gamma_{\boldsymbol{q}} - \gamma_{\boldsymbol{k}}), \tag{6}$$

where we defined $\gamma_{\boldsymbol{k}} = 2(\cos k_x + \cos k_y)$. Note that the Bogoliubov analysis can be generalized to next nearest neighbor interactions by modifying the definition of $\gamma_{\boldsymbol{k}}$

accordingly. From Eq.(6), we note that the value of μ is $\mu = \varepsilon_{\boldsymbol{q}}$. The frequencies of the Bogoliubov modes are

$$\omega_{\boldsymbol{k}} = \frac{\varepsilon_{\boldsymbol{q}+\boldsymbol{k}} - \varepsilon_{\boldsymbol{q}-\boldsymbol{k}}}{2} \pm \frac{1}{2}\sqrt{\Delta\varepsilon(\Delta\varepsilon + 2\Delta_{\boldsymbol{k}})}, \qquad (7)$$

where $\Delta\varepsilon = \varepsilon_{\boldsymbol{q}+\boldsymbol{k}} + \varepsilon_{\boldsymbol{q}-\boldsymbol{k}} - 2\varepsilon_{\boldsymbol{q}}$ can be interpreted as the kinetic energy cost of unbinding two quasiparticles from the macroscopically occupied mode $\boldsymbol{q}$. For large spiral wavevectors, $q_x, q_y > \pi/2$, $\Delta\varepsilon$ can be negative because of the negative mass of bare particles and gives rise to the previously studied modulational instability[3]. For $q_x, q_y < \pi/2$, however, $\Delta\varepsilon$ is strictly positive and the condition for the mode $S^+_{\boldsymbol{q}+\boldsymbol{k}}$ to be unstable (*i.e.*, $\omega''_{\boldsymbol{k}} = \mathrm{Im}[\omega_{\boldsymbol{k}}] \neq 0$) is given by

$$\varepsilon_{\boldsymbol{q}+\boldsymbol{k}} + \varepsilon_{\boldsymbol{q}-\boldsymbol{k}} - 2\varepsilon_{\boldsymbol{q}} + 2\Delta_{\boldsymbol{k}} < 0. \qquad (8)$$

It is instructive to analyze the condition (8) in the limit of small $\boldsymbol{q}$ and θ such that we can contrast it with the Landau instability. The initial spin spiral state can be interpreted as a macroscopically occupied state (*i.e.*, a quasicondensate) with wavevector q on top of the ferromagnetic ground state. Upon approaching the classical limit ($S \to \infty$) the magnon interaction vanishes as $1/S$. As a result, the spiral does not decay in the classical limit. At the isotropic point and for finite S, Eq.(8) reflects an energy balance condition resulting from unbinding two magnons of energy $\varepsilon_{\boldsymbol{q}\pm\boldsymbol{k}} \approx JSa^2(\boldsymbol{q} \pm \boldsymbol{k})^2$ and with a *momentum-dependent* pairing energy $\Delta_{\boldsymbol{k}} \approx -JSa^2 \sin^2\theta(\boldsymbol{q}^2 - \boldsymbol{k}^2)$. Importantly, $\Delta_{\boldsymbol{k}}$ is attractive in a ring of radius $|\boldsymbol{k}| \lesssim |\boldsymbol{q}|$. Attractive magnon-magnon interactions are known to give rise to magnon bound states in 1D[43] and its momentum dependence has been shown to result in unusual quasiparticle relaxation[44] and hydrodynamic behavior[45, 46]. Equation (8) dictates that, independently of S, the growth of modes with small wavevectors $\boldsymbol{k}$ relative to $\boldsymbol{q}$ is energetically favorable (a large value of $\boldsymbol{k}$, on the other hand, is penalized by a large kinetic energy cost, $\varepsilon_{\boldsymbol{q}+\boldsymbol{k}} + \varepsilon_{\boldsymbol{q}-\boldsymbol{k}} - 2\varepsilon_{\boldsymbol{q}} \propto \boldsymbol{k}^2$). In contrast, usual superfluids have a *repulsive* hard core interaction $\Delta_{\boldsymbol{k}} = gn > 0$ that is momentum independent, which means that the kinetic energy of the superfluid has to be sufficiently large (*i.e.*, there is a finite critical wavevector) for the instability criterion (8) to be satisfied (g: local interaction, n: density).

More generally, Eq.(8) gives rise to unstable modes for any value of $\boldsymbol{q}$ and θ. To analytically find the most unstable mode when $\boldsymbol{q} = (q_x, 0)$, we maximize $\omega''_{\boldsymbol{k}}$ under the constraint $k_x = 0$ [note that the fastest growing mode in Fig. 1(a) is transverse to $\boldsymbol{q}$]. In this case, we obtain

$$\omega''_{\boldsymbol{k}} = 2\sqrt{(1-\cos k_y)\left[(1-\cos k_y) - \sin^2\theta\,(1-\cos q_x)\right]}. \qquad (9)$$

From this, we see that the maximum of $\omega''_{\boldsymbol{k}}$ occurs at $k_y = \tilde{k}_y$, with $\tilde{k}_y$ satisfying $1-\cos\tilde{k}_y = \sin^2\theta(1-\cos q_x)/2$, and such mode grows with a rate $\max(\omega''_{\boldsymbol{k}}) = \frac{1}{\tau_*}$ in Eq.(1).

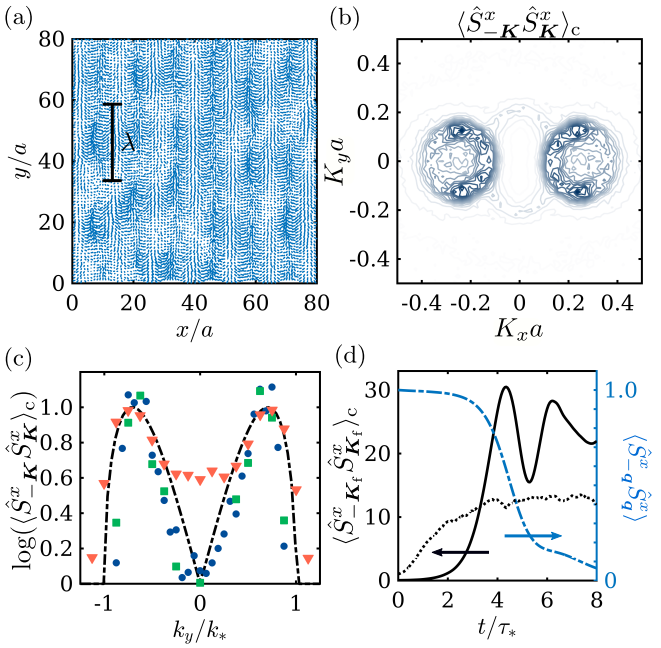


FIG. 2. Real space snapshot of a single TWA realization at $t/\tau_* = 3.5$, see Eq.(1). Shown are snapshots of the spins $\hat{\boldsymbol{S}}_j$ projected on the xy plane. Indicated with a bar is the wavelength in the y direction of the fastest growing mode. (b) Contour plot showing the connected correlation $\langle \hat{S}^x_{-\boldsymbol{K}} \hat{S}^x_{\boldsymbol{K}} \rangle_c$ corresponding to panel (a). Consistent with the Bogoliubov analysis, the plot exhibits a ring of unstable modes around $\boldsymbol{q}$ with size $k_* \approx q_x \sin\theta$ and a maximal amplitude transverse to $\boldsymbol{q}$. Parameters used in panel (a,b): $\theta = \pi/4$, $q_x = 0.25$, $q_y = 0$, $S = 10$ averaged over 50 realizations. (c) Spatial-temporal scaling of $\langle \hat{S}^x_{-\boldsymbol{K}} \hat{S}^x_{\boldsymbol{K}} \rangle_c$. Shown is the log of $\langle \hat{S}^x_{-\boldsymbol{K}} \hat{S}^x_{\boldsymbol{K}} \rangle_c$ for $\boldsymbol{K} = (q_x, k_y)$ and $t/\tau_* = 3.5$, and for different initial conditions: $(q_x, \theta) = (0.25, \pi/2)$ (circles), $(0.5, \pi/2)$ (squares) and $(0.25, \pi/4)$ (triangles) and $S = 10$. The dotted-dashed line is the Bogoliubov Im[ω] in Eq.(9) as a guide to the eye. (d) Growth of the most unstable mode, $\boldsymbol{K}_f = (q_x, \tilde{k}_y)$, showing saturation and subsequent oscillations for $S = 10$ (solid line) and $S = 1/2$ (dotted lines). Also shown is the depletion of the spin spiral (dashed-dotted line).

Equation (9) also defines the volume in phase space of unstable modes, which is bounded by the wavevector k_* satisfying the condition $1 - \cos k_* = \sin^2\theta[1 - \cos q_x]$. In the limit of small q_x, we obtain $\tilde{k}_y \approx k_*/\sqrt{2}$, with k_* defined in Eq.(1).

Phase space methods—To complement the Bogoliubov analysis, we compute real time dynamics of the spiral decay by incorporating quantum fluctuations using the Truncated Wigner Approximation[47]. Defining $\langle \hat{\boldsymbol{S}}^\perp_j \rangle$ as the transverse magnetization of the initial condition (3), we assume Gaussian fluctuations of $\hat{\boldsymbol{S}}^\perp_j$ given by $\langle \hat{\boldsymbol{S}}^\perp_j \rangle = 0$ and $\langle \hat{\boldsymbol{S}}^\perp_j \cdot \hat{\boldsymbol{S}}^\perp_j \rangle = S$.

Figure 2(a) shows a single realization of TWA noise for a spin spiral with parameters $\theta = \pi/4$ and $q_x = 0.5$ (same parameters as in Fig.1). Independently of the spin num-

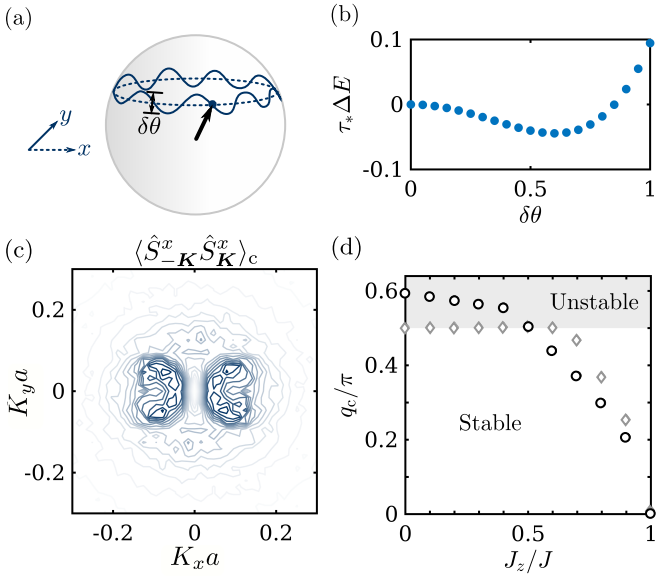


FIG. 3. (a) Schematics of the most favorable deformation of the spin spiral order and (b) the corresponding energy shift with respect to the spiral state. Shown in (a) is the trajectory of the magnetization vector by moving on the lattice in the x (dotted line) and y (solid line) directions, and $\delta\theta$ is the amplitude of deformation, see definition in main text. (c) Contour plot showing the connected component of $\langle \hat{S}^x_{-\boldsymbol{K}} \hat{S}^x_{\boldsymbol{K}} \rangle$ for $S = 1/2$, $q_x a = 0.12$, and $\theta = \pi/2$. (d) Stability boundary showing the critical momentum q_c as a function of exchange anisotropy for a spiral amplitude of $\theta = \pi/4$ (black circles), $\theta = 0.1$ (gray diamonds), and $S \to \infty$. The shaded area indicates the parameter space region of the modulational instability.

ber S, we consistently observe growth of unstable modes that lead to a disordered state. Analysis of the connected correlation $\langle \hat{S}^x_{-\boldsymbol{K}} \hat{S}^x_{\boldsymbol{K}} \rangle_c = \langle \hat{S}^x_{-\boldsymbol{K}} \hat{S}^x_{\boldsymbol{K}} \rangle - \langle \hat{S}^x_{-\boldsymbol{K}} \rangle \langle \hat{S}^x_{\boldsymbol{K}} \rangle$ [shown in Fig.2(b), with $\boldsymbol{K}$ the absolute wavevector] reveals that the spiral state is primarily decaying into modes located in a ring around the wavevector $\boldsymbol{q}$, preferentially in the direction perpendicular to $\boldsymbol{q}$, thus confirming the Bogoliubov analysis above.

In addition, Fig.2(c) shows the scaling of fluctuations for wavectors $\boldsymbol{K} = (q_x, k_y)$ and various initial conditions at the rescaled time $t/\tau_* = 3.5$. Given that we expect unstable modes to grow as $S^+_{\boldsymbol{K}}(t) \approx S^+_{\boldsymbol{K}}(0) e^{t/\tau_{\boldsymbol{K}}}$, the y axis is plotted in log scale and the correlation $\langle \hat{S}^x_{-\boldsymbol{K}} \hat{S}^x_{\boldsymbol{K}} \rangle_c$ is normalized with the maximum value as a function of k_y for each initial condition. We observe excellent agreement with the Bogoliubov analysis for all $\boldsymbol{q}$ and θ.

Instability growth and self-regularization—Going beyond the linear stability analysis, we inquire about the intermediate timescale dynamics of instability growth. Figure 2(d) shows the decay of the spin spiral and multiple stages in the evolution of the most unstable mode: (i) initial growth compatible with the Bogoliubov analysis above, (ii) saturation, (iii) coherent oscillations prior to equilibration. Unlike usual instabilities in BEC where unstable modes grow exponentially for long times, the local constraint $\hat{S}^2_j = S(S+1)$ and the conservation of total magnetization regulates the growth of the transverse spin modulation at relatively short times, analogously to Refs.[33, 48, and 49]. We observe that saturation occurs at $t \approx 4\tau_*$, irrespective of the value of S, $\boldsymbol{q}$ and θ (see Supplement).

The existence of unstable modes in the linearized analysis and the small oscillations in Fig.2(d) are linked to the existence of smooth, symmetry-allowed deformations of the spin spiral order with a valley-shaped potential. Using the insights gained from the Bogoliubov analysis, we propose a simple Ansatz for a transverse spin texture given by $S^\pm_j = S \sin\theta_i e^{\pm i \boldsymbol{q}\cdot\boldsymbol{r}_j}$ and $S^z_j = S\cos\theta_j$, with $\theta_j = \bar{\theta} + 2\delta\theta\cos(\tilde{k}_y y_i)$ and $\tilde{k}_y$ defined below Eq.(9) [see Fig.3(a)]. The value of $\delta\theta$ controls the amplitude of transverse spin deformations around $\bar{\theta}$ and is modulated by the transverse wavevector $\tilde{k}_y$. This ansatz trivially satisfies $\sum_j S^\pm_j = 0$ for all values of $\bar{\theta}$ and $\delta\theta$, and the condition $\frac{1}{N}\sum_j S^z_j = S\cos\theta$ defines a constraint that links $\bar{\theta}$ and $\delta\theta$. Because we recover Eq.(3) when $\bar{\theta} = \theta$ and $\delta\theta = 0$, our Ansatz is smoothly connected to the original spiral and preserves its total magnetization. Figure 3(b) shows that increasing the transverse modulation $\delta\theta$ reduces the energy of the spin spiral. In addition, the observed oscillations in Fig.2(d) can be interpreted as amplitude oscillations on a valley-shaped potential. The same argument can be applied to any value of $\boldsymbol{k}$ that satisfies the instability condition (8), but the valley is deepest for $\boldsymbol{K} = (q_x, \tilde{k}_y)$.

Crossover to the quantum regime— The stability analysis above relies on a $1/S$ expansion of the equations of motion, opening the question on its validity in the experimentally relevant $S = 1/2$ case. The competition between quantumness in the $S \to 1/2$ limit and classicality in the $\boldsymbol{q} \to 0$ limit suggests that a smeared, but still observable, ring of unstable modes is obtained for finite but small $\boldsymbol{q}$ and $S = 1/2$. Indeed, our numerics reveal that strong quantum fluctuations supress the exponential growth of unstable modes and smear out coherent oscillations in the two-point correlation function [see Fig.2(d)], but the latter still exhibits an imprint of the ring of unstable modes, see Fig.3(c). Remarkably, we also find that our stability analysis is valid in the one-dimensional Heisenberg model despite integrability and reduced dimensionality, as shown with Matrix Product States and TWA in the Supplement (in this case, the most unstable modes are necessarily collinear with q_x).

Crossover to modulational instability— To study the crossover between the transverse instability in the Heisenberg model ($J_z = J$) to the modulational instability that characterizes a superfluid on a lattice, we extend the Bogoliubov analysis for values of $J_z < J$ (see details in the Supplement). Tuning J_z can be realized

experimentally using Feshbach resonances, dipolar interactions or lattice shacking[50–54]. The anisotropic exchange energetically penalizes the transverse deformation of the spin spiral order. In the language of the stability condition in Eq.(8), the pairing $\Delta_{\boldsymbol{k}}$ becomes repulsive, $\Delta_{\boldsymbol{k}} \approx (J - J_z)$, and $\varepsilon_{\boldsymbol{k}}$ becomes linearly dispersing. Although reducing the SU(2) symmetry to U(1) has a stabilizing effect on the spin spiral state, there is still a strong reduction of the critical wavevector close to the SU(2) symmetric point, as shown in Fig.3(d). This suggests that the instability mechanism that we describe is also relevant for systems with weak anisotropic exchange.

Conclusions—We analyzed a new class of dynamic instability which is enabled by the topology of the order parameter manifold rather than kinematic effects. Such instability is an intrinsic mechanism that hinders long range phase coherence in spin systems. While the mechanism that we discuss is intrinsic to the Heisenberg model with ferromagnetic ordering, open problems include understanding the enhancement of the instability in the presence of disorder and long-range interactions, and understanding the mechanisms of decay in systems with antiferromagnetic ordering and different lattice types. In addition, extending our simulations to longer timescales in order to obtain a wholistic perspective of thermalization, which captures the growth of unstable modes and subsequent quasiparticle relaxation, remains an important challenge.

Acknowledgements—We thank Marin Bukov, Wen Wei Ho, Asier Piñeiro Orioli, Daniel Podolsky, Ana Maria Rey, Amir Yacoby, Tony Zhou and Bihui Zhu for valuable insights and discussions. JFRN acknowledges the Gordon and Betty Moore Foundations EPiQS Initiative through Grant GBMF4302 and GBMF8686, the 2019 KITP program *Spin and Heat Transport in Quantum and Topological Materials*, and the National Science Foundation under Grant No. NSF PHY-1748958. AS and MK acknowledge support from the Technical University of Munich - Institute for Advanced Study, funded by the German Excellence Initiative and the European Union FP7 under grant agreement 291763, the Max Planck Gesellschaft (MPG) through the International Max Planck Research School for Quantum Science and Technology (IMPRS-QST), the Deutsche Forschungsgemeinschaft (DFG, German Research Foundation) under Germany's Excellence Strategy–EXC–2111–390814868, DFG TRR80 and DFG grant No. KN1254/1-2, and from the European Research Council (ERC) under the European Union's Horizon 2020 research and innovation programme (grant agreement No. 851161). ED acknowledges support from the Harvard-MIT CUA, AFOSR-MURI: Photonic Quantum Matter (award FA95501610323), and the DARPA DRINQS program (award D18AC00014).

[1] L. Landau, Phys. Rev. **60**, 356 (1941).
[2] Z. Dutton, M. Budde, C. Slowe, and L. V. Hau, Science **293**, 663 (2001).
[3] B. Wu and Q. Niu, Phys. Rev. A **64**, 061603 (2001).
[4] L. Fallani, L. De Sarlo, J. E. Lye, M. Modugno, R. Saers, C. Fort, and M. Inguscio, Phys. Rev. Lett. **93**, 140406 (2004).
[5] A. Polkovnikov, E. Altman, E. Demler, B. Halperin, and M. D. Lukin, Phys. Rev. A **71**, 063613 (2005).
[6] E. Altman, A. Polkovnikov, E. Demler, B. I. Halperin, and M. D. Lukin, Phys. Rev. Lett. **95**, 020402 (2005).
[7] A. A. Norrie, R. J. Ballagh, and C. W. Gardiner, Phys. Rev. Lett. **94**, 040401 (2005).
[8] H. Takeuchi, S. Ishino, and M. Tsubota, Phys. Rev. Lett. **105**, 205301 (2010).
[9] R. W. Cherng, V. Gritsev, D. M. Stamper-Kurn, and E. Demler, Phys. Rev. Lett. **100**, 180404 (2008).
[10] R. W. Cherng and E. Demler, Phys. Rev. Lett. **103**, 185301 (2009).
[11] K. Fujimoto and M. Tsubota, Phys. Rev. A **85**, 033642 (2012).
[12] J. S. Langer and V. Ambegaokar, Phys. Rev. **164**, 498 (1967).
[13] D. E. McCumber and B. I. Halperin, Phys. Rev. B **1**, 1054 (1970).
[14] D. E. Sheehy and P. M. Goldbart, Phys. Rev. B **57**, R8131 (1998).
[15] B. I. Halperin, G. Refael, and E. Demler, International Journal of Modern Physics B **24**, 4039 (2010).
[16] T. Paul, P. Schlagheck, P. Leboeuf, and N. Pavloff, Phys. Rev. Lett. **98**, 210602 (2007).
[17] M. Albert, T. Paul, N. Pavloff, and P. Leboeuf, Phys. Rev. Lett. **100**, 250405 (2008).
[18] M. Albert, T. Paul, N. Pavloff, and P. Leboeuf, Phys. Rev. A **82**, 011602 (2010).
[19] T. Haga and M. Ueda, "Anomalous phase fluctuations of a superfluid flowing in a random potential," (2019), arXiv:arXiv:1909.11997 [cond-mat.quant-gas].
[20] L. Santos, G. V. Shlyapnikov, P. Zoller, and M. Lewenstein, Phys. Rev. Lett. **85**, 1791 (2000).
[21] K. Góral and L. Santos, Phys. Rev. A **66**, 023613 (2002).
[22] L. Santos, G. V. Shlyapnikov, and M. Lewenstein, Phys. Rev. Lett. **90**, 250403 (2003).
[23] G. Bertotti, I. Mayergoyz, and C. Serpico, Physica B: Condensed Matter **306**, 106 (2001), proceedings of the Third International Symposium on Hysteresis an d Micromagnetics Modeling.
[24] A. J. E. Kreil, D. A. Bozhko, H. Y. Musiienko-Shmarova, V. I. Vasyuchka, V. S. L'vov, A. Pomyalov, B. Hillebrands, and A. A. Serga, Phys. Rev. Lett. **121**, 077203 (2018).
[25] K. Wintersperger, M. Bukov, J. Nger, S. Lellouch, E. Demler, U. Schneider, I. Bloch, N. Goldman, and M. Aidelsburger, "Parametric instabilities of interacting bosons in periodically-driven 1d optical lattices," (2018), arXiv:1808.07462 [cond-mat.quant-gas].
[26] M. Bukov, S. Gopalakrishnan, M. Knap, and E. Demler, Phys. Rev. Lett. **115**, 205301 (2015).
[27] T. Boulier, J. Maslek, M. Bukov, C. Bracamontes, E. Magnan, S. Lellouch, E. Demler, N. Goldman, and J. V. Porto, Phys. Rev. X **9**, 011047 (2019).

[28] A. B. Bardon, S. Beattie, C. Luciuk, W. Cairncross, D. Fine, N. S. Cheng, G. J. A. Edge, E. Taylor, S. Zhang, S. Trotzky, and J. H. Thywissen, Science **344**, 722 (2014).

[29] S. Hild, T. Fukuhara, P. Schauß, J. Zeiher, M. Knap, E. Demler, I. Bloch, and C. Gross, Phys. Rev. Lett. **113**, 147205 (2014).

[30] R. C. Brown, R. Wyllie, S. B. Koller, E. A. Goldschmidt, M. Foss-Feig, and J. V. Porto, Science **348**, 540 (2015).

[31] M. Tsubota, Journal of Physics: Condensed Matter **21**, 164207 (2009).

[32] J. F. Rodriguez-Nieva, Phys. Rev. B **104**, L060302 (2021).

[33] M. Babadi, E. Demler, and M. Knap, Phys. Rev. X **5**, 041005 (2015).

[34] A. Piñeiro Orioli, K. Boguslavski, and J. Berges, Phys. Rev. D **92**, 025041 (2015).

[35] J. Berges, arXiv e-prints , arXiv:1503.02907 (2015).

[36] N. Jepsen, J. Amato-Grill, I. Dimitrova, W. W. Ho, E. Demler, and W. Ketterle, Nature **588**, 403 (2020).

[37] E. Sonin, Advances in Physics **59**, 181 (2010).

[38] D. A. Bozhko, A. A. Serga, P. Clausen, V. I. Vasyuchka, F. Heussner, G. A. Melkov, A. Pomyalov, V. S. Lvov, and B. Hillebrands, Nature Physics **12**, 1057 (2016).

[39] S. Takei and Y. Tserkovnyak, Phys. Rev. Lett. **112**, 227201 (2014).

[40] K. Nakata, K. A. van Hoogdalem, P. Simon, and D. Loss, Phys. Rev. B **90**, 144419 (2014).

[41] C. Sun, T. Nattermann, and V. L. Pokrovsky, Phys. Rev. Lett. **116**, 257205 (2016).

[42] E. B. Sonin, Phys. Rev. B **95**, 144432 (2017).

[43] D. C. Mattis, *The Theory of Magnetism Made Simple* (WORLD SCIENTIFIC, 2006).

[44] S. Bhattacharyya, J. F. Rodriguez-Nieva, and E. Demler, Phys. Rev. Lett. **125**, 230601 (2020).

[45] E. Iacocca, T. J. Silva, and M. A. Hoefer, Phys. Rev. Lett. **118**, 017203 (2017).

[46] J. F. Rodriguez-Nieva, D. Podolsky, and E. Demler, "Hydrodynamic sound modes and galilean symmetry breaking in a magnon fluid," (2018), arXiv:1810.12333 [cond-mat.mes-hall].

[47] A. Polkovnikov, Annals of Physics **325**, 1790 (2010).

[48] J. Berges and J. Serreau, Phys. Rev. Lett. **91**, 111601 (2003).

[49] J. Berges, A. Rothkopf, and J. Schmidt, Phys. Rev. Lett. **101**, 041603 (2008).

[50] S. Trotzky, P. Cheinet, S. Fölling, M. Feld, U. Schnorrberger, A. M. Rey, A. Polkovnikov, E. A. Demler, M. D. Lukin, and I. Bloch, Science **319**, 295 (2008).

[51] B. Yan, S. A. Moses, B. Gadway, J. P. Covey, K. R. A. Hazzard, A. M. Rey, D. S. Jin, and J. Ye, Nature **501**, 521 (2013).

[52] C. V. Parker, L.-C. Ha, and C. Chin, Nature Physics **9**, 769 (2013).

[53] C.-L. Hung, A. González-Tudela, J. I. Cirac, and H. J. Kimble, Proceedings of the National Academy of Sciences **113**, E4946 (2016), https://www.pnas.org/content/113/34/E4946.full.pdf.

[54] E. J. Davis, G. Bentsen, L. Homeier, T. Li, and M. H. Schleier-Smith, Phys. Rev. Lett. **122**, 010405 (2019).